Eur. Phys. J. C (2017) 77:221
DOI 10.1140/epjc/s10052-017-4770-4

THE EUROPEAN PHYSICAL JOURNAL C

Regular Article - Theoretical Physics

Is the color-octet mechanism consistent with the double J/ψ production measurement at B-factories?

Yu Feng[1], **Zhan Sun**[2,a], **Hong-Fei Zhang**[1,3,b]

[1] Department of Physics, School of Biomedical Engineering, Third Military Medical University, Chongqing 400038, People's Republic of China
[2] School of Science, Guizhou Minzu University, Guiyang 550025, People's Republic of China
[3] School of Science, Chongqing University of Posts and Telecommunications, Chongqing, People's Republic of China

Received: 4 January 2017 / Accepted: 19 March 2017 / Published online: 8 April 2017

Abstract Double J/ψ production in e^+e^- collisions involving color-octet channels are evaluated up to order $\alpha^2\alpha_s^3$. Having implemented the variation of the parameters (m_c, μ_r and long-distance matrix elements), we found that the cross sections for producing double J/ψ at B-factories range from -0.016 to 0.245 fb, which are even much smaller than that via the color-singlet mechanism. Accordingly, this result is consistent with the measurement by the Belle and BABAR Collaborations.

1 Introduction

The phenomenological study of the nonrelativistic QCD (NRQCD) effective theory [1] is making progress since the LHC started its running. Copious data not only provides evidence for the color-octet (CO) mechanism, but it also indicates challenges to the theory. In addition to the fact that the J/ψ hadroproduction data can be well reproduced by the theoretical evaluations within the NRQCD framework [2–4], χ_c hadroproduction [5,6] gives other strong support. In the low transverse momentum (p_t) region, even though the factorization might not hold, the color-glass-condensate model [7–9] associated with NRQCD [10] did a good job in the description of the J/ψ production in proton–proton and proton–nucleus collisions [11,12]. Despite all the successes, we cannot overlook the challenges it is facing. The universality of the NRQCD long-distance matrix elements (LDMEs) has not yet been suggested in all the processes. As an example, the constraint [13] on the CO LDMEs indicated by the QCD next-to-leading order (NLO) study of the J/ψ production at B-factories is apparently below the LDME values obtained through the fit of the J/ψ production data at other colliders [3,14–16]. The perspectives of the long-standing J/ψ polarization puzzle still have not converged. Three groups [15,17,18] achieved the calculation of the J/ψ polarization at hadron colliders at QCD NLO; however, with different LDMEs, their results are completely different from one another. Recently, the η_c hadroproduction was measured by the LHCb Collaboration [19], which provides another laboratory for the study of NRQCD. Ref. [20] considers it as a challenge to NRQCD, while Refs. [21,22] found this data to be consistent with the J/ψ hadroproduction measurements. Further, with the constraint on the LDMEs obtained in Refs. [22,23] discovered some interesting features of the J/ψ polarization, and found a possibility of understanding the J/ψ polarization within the NRQCD framework.

The J/ψ pair production at B-factories is another challenge that NRQCD is facing. The Belle [24] and BABAR [25] Collaborations observed the process $e^+e^- \to J/\psi$+charmonium, and found no evidence for the J/ψ pair events, while the QCD leading order (LO) calculation based on the color-singlet (CS) mechanism predicted a significant production rate [26–29]. This was understood by the QCD NLO corrections [30], which contribute a negative value and cancel the large LO cross sections. Reference [31] studied the resummation of the relativistic corrections to double J/ψ production at B-factories, and one found that their results are also consistent with the measurements. Reference [30] only addressed the CS contributions. However, the Belle and BABAR measurements actually did not exclude the double J/ψ plus light hadron events. Both of the experiments measured the $M_{\rm res}$ spectrum, where $M_{\rm res}$ denotes the invariant mass of all the final states except for the fully reconstructed J/ψ. These distributions exhibited no significant excess in the range of about 300 MeV above the J/ψ mass, which suggested that the cross section for the J/ψ pair plus light hadron (e.g. π^0, $\pi^+\pi^-$) associated production is also too small to observe. To accord with NRQCD, the double J/ψ

[a] e-mail: zhansun@cqu.edu.cn
[b] e-mail: hfzhang@ihep.ac.cn

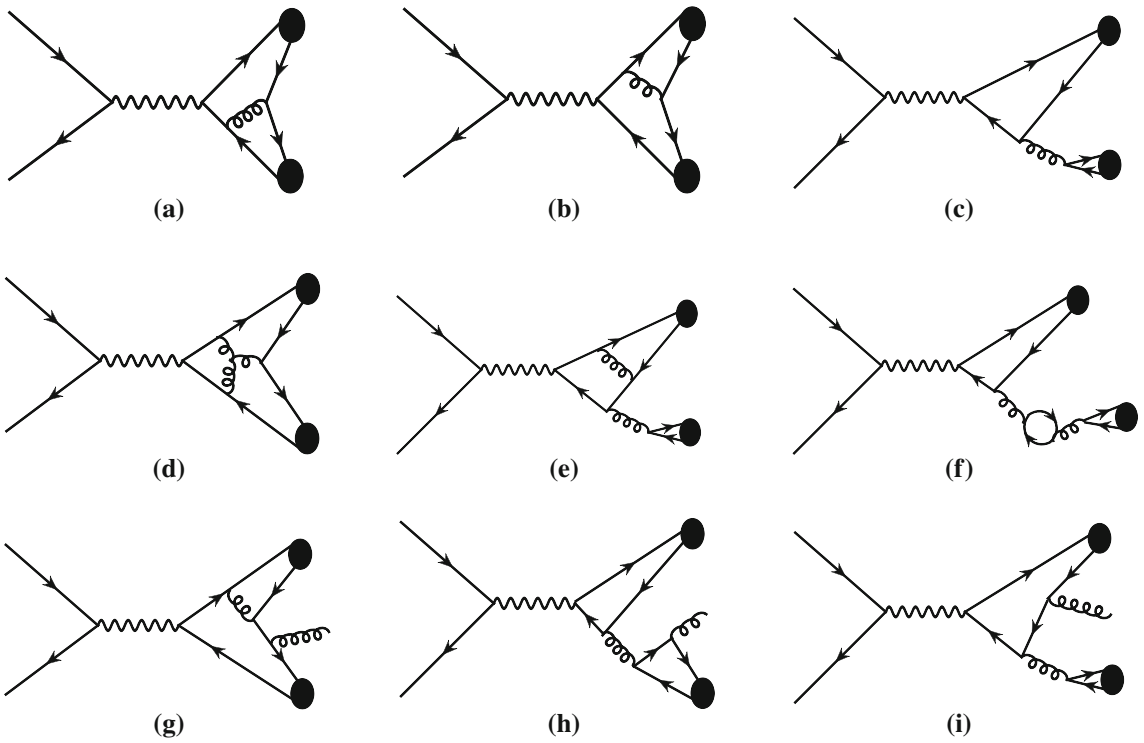

Fig. 1 Representative Feynman diagrams

production cross sections involving the CO channels must not be significant, which, however, is not manifest. Although suppressed by the CO LDMEs, the double J/ψ yield due to the CO mechanism is enhanced by the powers of α_s/α, relative to via the CS channels. As is pointed out in Refs. [26,30], at B-factories, double $c\bar{c}({}^3S_1^{[1]})$ can be produced via two virtual photons generated through e^+e^- annihilation, and the LO contribution is of order $\mathcal{O}(\alpha^4\alpha_s^0)$. In contrast, as illustrated in Fig. 1a–c), the diagrams for the processes

$$e^+e^- \to c\bar{c}(m_1) + c\bar{c}(m_2), \tag{1}$$

when n_1 and n_2 have the opposite charge conjugation, involve only a single virtual photon, and the LO contribution is of order $\mathcal{O}(\alpha^2\alpha_s^2)$. For double J/ψ production, m_1 and m_2 have only two possible configurations, which are $m_1 = {}^3S_1^{[8]}$ and $m_2 = {}^1S_0^{[8]}$, and $m_1 = {}^3S_1^{[8]}$ and $m_2 = {}^3P_J^{[8]}$. These two processes are suppressed by the CO LDMEs by a factor of $v^8 \approx 0.002$, where v is the typical charm-quark velocity in the charmonium rest frame, however, enhanced by the coupling constants by a factor of $\alpha_s^2/\alpha^2 \approx 1000$, relative to via the CS channels. The double J/ψ can also be produced through such a kind of process,

$$e^+e^- \to c\bar{c}(n_1) + c\bar{c}(n_2) + g, \tag{2}$$

where g denotes a gluon. When $n_1 = {}^3S_1^{[1]}$ and $n_2 = {}^3S_1^{[8]}$ (or equivalently $n_1 = {}^3S_1^{[8]}$ and $n_2 = {}^3S_1^{[1]}$), this kind of processes is enhanced by the coupling constants by a factor of $\alpha_s^3/\alpha^2 \approx 200$ and reduced by the CO LDME by a factor of $v^4 \approx 0.05$, relative to the processes involving only the CS channels. In sum, the processes involving CO states are enhanced by a synthetic factor of about 2–10, compared with the processes considered in Refs. [26,30], the LO cross sections of which is large enough to be observed by Belle and BABAR experiments. Accordingly, we need to calculate the cross sections for the J/ψ pair production involving the CO channels to see whether NRQCD can endure this paradox.

In this work, we will present a comprehensive study of the double J/ψ production in e^+e^- annihilation involving CO channels up to order $\mathcal{O}(\alpha^2\alpha_s^3)$, and we check whether it is consistent with the measurements by Belle and BABAR Collaborations. The J/ψ plus χ_c production at B-factories has already been studied in Refs. [32–34], and their results do not contradict the double J/ψ measurements by Belle and BABAR Collaborations, regarding the branching ratios $\mathcal{B}(\chi_{c[0,1,2]} \to J/\psi) = [1.27, 33.9, 19.2\%]$ [35]. In this paper, we do not calculate the $c\bar{c}({}^3S_1^{[1]}) + c\bar{c}({}^3P_J^{[1]})$ production. We also notice that the J/ψ may come from the χ_{cJ} feed down, where the χ_{cJ} can be produced via the ${}^3S_1^{[8]}$ channel. By employing the LDMEs obtained in Refs. [6,23], $\langle O^{\chi_{c0}}({}^3S_1^{[8]})\rangle = 2.01 \times 10^{-3}\ \mathrm{GeV}^3$ and $\langle O^{J/\psi}({}^3S_1^{[8]})\rangle = 1.08 \times 10^{-2}\ \mathrm{GeV}^3$ in association with the branching ratios listed above, we find that this contribution is much smaller than that from the J/ψ directly produced through the ${}^3S_1^{[8]}$

Table 1 Possible Feynman diagrams for each of the final-state-gluon-emission processes. The processes are abbreviated to the numbers of the equations, namely Eqs. (4), (5), (6), (7), (8), (9), in which the processes are presented

Process	(4)	(5)	(6)	(7)	(8)	(9)
Feynman diagrams	Figure 1g–i	Figure 1g, i	Figure 1g, h	Figure 1g, i	Figure 1g, h	Figure 1g, h

channel. Similarly, the J/ψ production cross sections via the $\psi(2s)$ feed down is also smaller than that for the directly produced ones. For this reason, we completely omit the discussions on the feed down contributions from both χ_c and $\psi(2s)$.

The rest of this paper is organized as follows. In Sect. 2, we outline the formalism of the calculation. Section 3 presents the numerical results and related discussions, followed by a concluding remark in Sect. 4.

2 Double J/ψ production in NRQCD framework

Following the NRQCD factorization, the total cross sections for the J/ψ pair production can be expressed as

$$\begin{aligned}\sigma(e^+e^- \to J/\psi + J/\psi + X) &= \sum_{n_1,n_2} \hat{\sigma}(e^+e^- \to c\bar{c}(n_1) + c\bar{c}(n_2) + X) \\ &\times \langle O^{J/\psi}(n_1)\rangle \langle O^{J/\psi}(n_2)\rangle, \end{aligned} \tag{3}$$

where n_1, n_2 run over all the possible configurations of the $c\bar{c}$ intermediate states with certain color and angular momentum, $\hat{\sigma}$ is the short-distance coefficient (SDC), and $\langle O^{J/\psi}(n_1)\rangle$ and $\langle O^{J/\psi}(n_2)\rangle$ are the corresponding LDMEs. When at least one of n_1 and n_2 is a CO state, the LO contributions are of order $\mathcal{O}(\alpha_s^2\alpha^2)$. At this order, all the processes have the form of Eq. (1), in which the only possible configurations of m_1 and m_2 are $m_1 = {}^3S_1^{[8]}$, $m_2 = {}^1S_0^{[8]}$ and $m_1 = {}^3S_1^{[8]}$, $m_2 = {}^3P_J^{[8]}$, and the representative Feynman diagrams are illustrated in Fig. 1a–c. At QCD NLO ($\mathcal{O}(\alpha_s^3\alpha^2)$), in addition to the virtual corrections (the representative Feynman diagrams for which are shown in Fig. 1d–f) to the processes presented in Eq. (1), double $c\bar{c}$ states in association with a gluon production are also required for consideration, as illustrated in Eq. (2). The real-correction processes to the LO ones are

$$\begin{aligned} e^+e^- &\to c\bar{c}({}^3S_1^{[8]}) + c\bar{c}({}^1S_0^{[8]}) + g, \\ e^+e^- &\to c\bar{c}({}^3S_1^{[8]}) + c\bar{c}({}^3P_J^{[8]}) + g, \end{aligned} \tag{4}$$

in addition to which five processes are also at this order, as listed below, and they will be calculated in our paper. We have

$$e^+e^- \to c\bar{c}({}^3S_1^{[1]}) + c\bar{c}({}^3S_1^{[8]}) + g, \tag{5}$$

$$e^+e^- \to c\bar{c}({}^1S_0^{[8]}) + c\bar{c}({}^1S_0^{[8]}) + g, \tag{6}$$

$$e^+e^- \to c\bar{c}({}^3S_1^{[8]}) + c\bar{c}({}^3S_1^{[8]}) + g, \tag{7}$$

$$e^+e^- \to c\bar{c}({}^1S_0^{[8]}) + c\bar{c}({}^3P_J^{[8]}) + g, \tag{8}$$

$$e^+e^- \to c\bar{c}({}^3P_J^{[8]}) + c\bar{c}({}^3P_J^{[8]}) + g. \tag{9}$$

The representative Feynman diagrams for the final-state-gluon-emission processes are presented in Fig. 1g–i. However, not all the processes have the three types of diagrams. So, we summarize the possible diagrams for each of the processes in Table 1.

Before we present the numerical results, we first address the divergences rising from the processes listed above. First of all, the LO processes are divergence free, and we denote their total cross sections as $\sigma^{LO} = \sigma^{LO}_{{}^3S_1^{[8]}+{}^1S_0^{[8]}} + \sigma^{LO}_{{}^3S_1^{[8]}+{}^3P_J^{[8]}}$. The virtual corrections to σ^{LO} contain both ultraviolet (UV) and infrared (IR) divergences. The UV divergences can be eliminated through the renormalization procedure, while the IR divergences will be canceled by those emerging in the real corrections, the processes for which are presented in Eq. (4). We denote the renormalized virtual-correction total cross sections as $\sigma^V = \sigma^V_{{}^3S_1^{[8]}+{}^1S_0^{[8]}} + \sigma^V_{{}^3S_1^{[8]}+{}^3P_J^{[8]}}$, and the real corrections to σ^{LO} as $\sigma^R = \sigma^R_{{}^3S_1^{[8]}+{}^1S_0^{[8]}} + \sigma^R_{{}^3S_1^{[8]}+{}^3P_J^{[8]}}$. The complete QCD NLO corrections to σ^{LO} can be expressed as

$$\sigma^{NLO} \equiv \sigma^V + \sigma^R = \sigma^{NLO}_{{}^3S_1^{[8]}+{}^1S_0^{[8]}} + \sigma^{NLO}_{{}^3S_1^{[8]}+{}^3P_J^{[8]}}, \tag{10}$$

where

$$\begin{aligned} \sigma^{NLO}_{{}^3S_1^{[8]}+{}^1S_0^{[8]}} &= \sigma^V_{{}^3S_1^{[8]}+{}^1S_0^{[8]}} + \sigma^R_{{}^3S_1^{[8]}+{}^1S_0^{[8]}}, \\ \sigma^{NLO}_{{}^3S_1^{[8]}+{}^3P_J^{[8]}} &= \sigma^V_{{}^3S_1^{[8]}+{}^3P_J^{[8]}} + \sigma^R_{{}^3S_1^{[8]}+{}^3P_J^{[8]}}. \end{aligned} \tag{11}$$

Both $\sigma^{NLO}_{{}^3S_1^{[8]}+{}^1S_0^{[8]}}$ and $\sigma^{NLO}_{{}^3S_1^{[8]}+{}^3P_J^{[8]}}$ are divergence free. The total cross sections for the J/ψ pair production through ${}^3S_1^{[8]} + {}^1S_0^{[8]}$ and ${}^3S_1^{[8]} + {}^3P_J^{[8]}$ channels are the sum of their LO and NLO contributions.

$$\begin{aligned} \sigma_{{}^3S_1^{[8]}+{}^1S_0^{[8]}} &= \sigma^{LO}_{{}^3S_1^{[8]}+{}^1S_0^{[8]}} + \sigma^{NLO}_{{}^3S_1^{[8]}+{}^1S_0^{[8]}}, \\ \sigma_{{}^3S_1^{[8]}+{}^3P_J^{[8]}} &= \sigma^{LO}_{{}^3S_1^{[8]}+{}^3P_J^{[8]}} + \sigma^{NLO}_{{}^3S_1^{[8]}+{}^3P_J^{[8]}}. \end{aligned} \tag{12}$$

Note that we adopt the on-shell (OS) renormalization scheme for the renormalization of c-quark mass and the wave func-

tions of the c-quark and gluon, and the modified-minimum-subtraction ($\overline{MS}$) scheme for that of the QCD coupling constant, which coincide with Ref. [36]. The corresponding renormalization constants, Z_m^{OS} (for the c-quark mass), Z_2^{OS} (for the c-quark wave function), Z_3^{OS} (for the gluon wave function), and $Z_g^{\overline{MS}}$ (for the QCD coupling constant), are

$$\begin{aligned}
\delta Z_m^{OS} &= -3C_F\frac{\alpha_s}{4\pi}\left[\frac{1}{\epsilon_{UV}} - \gamma_E + \ln\frac{4\pi\mu_r^2}{m_c^2} + \frac{4}{3}\right],\\
\delta Z_2^{OS} &= -C_F\frac{\alpha_s}{4\pi}\left[\frac{1}{\epsilon_{UV}} + \frac{2}{\epsilon_{IR}} - 3\gamma_E + 3\ln\frac{4\pi\mu_r^2}{m_c^2} + 4\right],\\
\delta Z_3^{OS} &= \frac{\alpha_s}{4\pi}\left[(\beta_0' - 2C_A)\left(\frac{1}{\epsilon_{UV}} - \frac{1}{\epsilon_{IR}}\right)\right.\\
&\quad \left. - \frac{4}{3}T_F\left(\frac{1}{\epsilon_{UV}} - \gamma_E + \ln\frac{4\pi\mu_r^2}{m_c^2}\right)\right],\\
\delta Z_g^{\overline{MS}} &= -\frac{\beta_0}{2}\frac{\alpha_s}{4\pi}\left[\frac{1}{\epsilon_{UV}} - \gamma_E + \ln(4\pi)\right],
\end{aligned} \tag{13}$$

where μ_r is the renormalization scale, γ_E is Euler's constant, $\beta_0 = \frac{11}{3}C_A - \frac{4}{3}T_F n_f$ is the one-loop coefficient of the QCD beta function, n_f is the number of active quark flavors. In SU(3)$_c$, color factors are given by $T_F = \frac{1}{2}, C_F = \frac{4}{3}, C_A = 3$, and $\beta_0' \equiv \beta_0 + (4/3)T_F = (11/3)C_A - (4/3)T_F n_{lf}$, where $n_{lf} \equiv n_f - 1 = 3$ is the number of light quark flavors. Actually, in the NLO total amplitude level, the terms proportional to δZ_3^{OS} cancel each other; thus the result is independent of the renormalization scheme of the gluon field.

The cross sections for the processes listed in Eqs. (8) and (9) also have divergences, which, however, can be eliminated through the renormalization of the SDCs for them. We take the process (8) as an example. The cancellation of its divergences requires the calculation of the NLO corrections to $\langle O^{J/\psi}(^3S_1^{[8]})\rangle$. The bare LDME can be expressed as

$$\begin{aligned}
\langle O^{J/\psi}(^3S_1^{[8]})\rangle_{\text{bare}} &= \langle O^{J/\psi}(^3S_1^{[8]})\rangle - \frac{\alpha_s}{\pi m_c^2}\frac{N_c^2-4}{N_c}\\
&\quad\times\left(\frac{1}{\epsilon_{IR}} - \frac{1}{\epsilon_{UV}}\right)\langle O^{J/\psi}(^3P_0^{[8]})\rangle,
\end{aligned} \tag{14}$$

where m_c is the c-quark mass, and $N_c = 3$ for SU(3) gauge theory. Here we adopt the μ_Λ-cutoff renormalization scheme [6] to subtract the UV divergence. By substituting the relation between the bare and renormalized LDMEs,

$$\begin{aligned}
&\langle O^{J/\psi}(^3S_1^{[8]})\rangle_{\text{bare}}\\
&= \langle O^{J/\psi}(^3S_1^{[8]})\rangle_{\text{renorm}} + \frac{\alpha_s}{\pi m_c^2}\frac{N_c^2-4}{N_c}\\
&\quad\times\left(\frac{1}{\epsilon_{UV}} - \gamma_E + \frac{5}{3} + ln\left(\frac{\pi\mu^2}{\mu_\Lambda^2}\right)\right)\langle O^{J/\psi}(^3P_0^{[8]})\rangle,
\end{aligned} \tag{15}$$

into Eq. (14), we obtain the renormalized LDME as

$$\begin{aligned}
&\langle O^{J/\psi}(^3S_1^{[8]})\rangle_{renorm}\\
&= \langle O^{J/\psi}(^3S_1^{[8]})\rangle - \frac{\alpha_s}{\pi m_c^2}\frac{N_c^2-4}{N_c}\\
&\quad\times\left(\frac{1}{\epsilon_{IR}} - \gamma_E + \frac{5}{3} + ln\left(\frac{\pi\mu^2}{\mu_\Lambda^2}\right)\right)\langle O^{J/\psi}(^3P_0^{[8]})\rangle.
\end{aligned} \tag{16}$$

Then process $e^+e^- \to c\bar{c}(^3S_1^{[8]}) + c\bar{c}(^1S_0^{[8]})$ contributes an additional divergent term,

$$\begin{aligned}
&\sigma_{div}(e^+e^- \to c\bar{c}(^3S_1^{[8]}) + c\bar{c}(^1S_0^{[8]}))\\
&= -\frac{\alpha_s}{\pi m_c^2}\frac{N_c^2-4}{N_c}\left(\frac{1}{\epsilon_{IR}} - \gamma_E + \frac{5}{3} + ln\left(\frac{\pi\mu^2}{\mu_\Lambda^2}\right)\right)\\
&\quad\times\hat{\sigma}(e^+e^- \to c\bar{c}(^3S_1^{[8]}) + c\bar{c}(^1S_0^{[8]}))\langle O^{J/\psi}(^3P_0^{[8]})\rangle,
\end{aligned} \tag{17}$$

which cancels the IR singularities arising from the process (8). In this sense, we can redefine the SDC for the process (8) as

$$\begin{aligned}
&\hat{\sigma}_{\text{renorm}}(e^+e^- \to c\bar{c}(^1S_0^{[8]}) + c\bar{c}(^3P_J^{[8]}) + g)\\
&= \hat{\sigma}(e^+e^- \to c\bar{c}(^1S_0^{[8]}) + c\bar{c}(^3P_J^{[8]}) + g)\\
&\quad - \frac{\alpha_s}{\pi m_c^2}\frac{N_c^2-4}{N_c}\left(\frac{1}{\epsilon_{IR}} - \gamma_E + \frac{5}{3} + ln\left(\frac{\pi\mu^2}{\mu_\Lambda^2}\right)\right)\\
&\quad\times\hat{\sigma}(e^+e^- \to c\bar{c}(^3S_1^{[8]}) + c\bar{c}(^1S_0^{[8]})),
\end{aligned} \tag{18}$$

where

$$\begin{aligned}
&\hat{\sigma}(e^+e^- \to c\bar{c}(^1S_0^{[8]}) + c\bar{c}(^3P_J^{[8]}) + g)\\
&= \hat{\sigma}(e^+e^- \to c\bar{c}(^1S_0^{[8]}) + c\bar{c}(^3P_0^{[8]}) + g)\\
&\quad + 3\hat{\sigma}(e^+e^- \to c\bar{c}(^1S_0^{[8]}) + c\bar{c}(^3P_1^{[8]}) + g)\\
&\quad + 5\hat{\sigma}(e^+e^- \to c\bar{c}(^1S_0^{[8]}) + c\bar{c}(^3P_2^{[8]}) + g)
\end{aligned} \tag{19}$$

has been implicated in Eq. (18) (the same convention applies to the SDCs with the subscript "renorm"). $\hat{\sigma}_{\text{renorm}}$ is a finite quantity, therefore, we can replace, in Eq. (3), the divergent one by it. The same operation can be done for the process (9) as well. Then we denote all the divergence-free total cross sections for the processes listed in Eqs. (5), (6), (7), (8), (9) as $\sigma_{n_1+n_2}$, where n_1 and n_2 are the corresponding $c\bar{c}$ states.

3 Numerical results

In our analytic calculation, we use our *Mathematica* package with the employment of FeynArts [37], FeynCalc [38], FIRE [39] and Apart [40]. As a cross check, we also compute the processes using the FDC package [41], except for the process (9). To subtract the IR divergences in the gluon-emission

Table 2 The values of $\hat{\sigma}_{n_1+n_2}$ in (fb/GeV^6) up to order $\mathcal{O}(\alpha^2\alpha_s^3)$. The convention introduced in Eq. (19) is adopted labeltab

n_2/n_1	$^3S_1^{[1]}$	$^1S_0^{[8]}$	$^3S_1^{[8]}$	$^3P_J^{[8]}$
$^3S_1^{[1]}$	0	0	4.55	0
$^1S_0^{[8]}$	0	0.28	167	−74.4
$^3S_1^{[8]}$	4.55	167	2.48	816
$^3P_J^{[8]}$	0	−74.4	816	−233

Table 3 The values of $\sigma_{n_1+n_2}$ in (fb) up to order $\mathcal{O}(\alpha^2\alpha_s^3)$. The convention introduced in Eq. (19) is adopted. The LDMEs are taken from Refs. [22,23]

n_2/n_1	$^3S_1^{[1]}$	$^1S_0^{[8]}$	$^3S_1^{[8]}$	$^3P_J^{[8]}$
$^3S_1^{[1]}$	0	0	0.032	0
$^1S_0^{[8]}$	0	1.68×10^{-5}	0.014	−0.012
$^3S_1^{[8]}$	0.032	0.014	2.90×10^{-4}	0.177
$^3P_J^{[8]}$	0	−0.012	0.177	−0.094

processes, we adopt the two-cutoff slicing strategy [42]. The independence of the cutoff has been checked.

We have the following global choices of the parameters in our calculation: $\alpha = 1/137$, and the colliding energy of the electron and positron is $\sqrt{s} = 10.6$ GeV. The J/ψ mass is fixed to $M_{J/\psi} = 2m_c$ to keep the gauge invariance. The default values of m_c and the renormalization scale (μ_r) are $m_c = 1.5$ GeV and $\mu_r = 3.0$ GeV, respectively. Since we investigate the μ_r dependence of the total cross sections, the two-loop running α_s is employed in our computation. The values of the SDCs for all the processes are listed in Table 2, where the SDCs for the $^3P_J^{[8]}$ channels are defined by multiplying a factor of m_c^2 to those defined in Ref. [1], in order to keep the homogeneity of the dimensions (for double $^3P_J^{[8]}$ production, this factor should be m_c^4). The LO SDCs for $^1S_0^{[8]} +^3 S_1^{[8]}$ and $^3S_1^{[8]} +^3 P_J^{[8]}$ productions are 60.07 and 290.9 fb/GeV^6, respectively.

Employing the LDMEs obtained in Refs. [22,23], namely

$$\begin{aligned}
&\langle O^{J/\psi}(^3S_1^{[1]})\rangle = 0.65\ \text{GeV}^3\\
&\langle O^{J/\psi}(^1S_0^{[8]})\rangle = 0.78\times10^{-2}\ \text{GeV}^3\\
&\langle O^{J/\psi}(^3S_1^{[8]})\rangle = 1.08\times10^{-2}\ \text{GeV}^3\\
&\langle O^{J/\psi}(^3P_0^{[8]})\rangle/m_c^2 = 2.01\times10^{-2}\ \text{GeV}^3
\end{aligned} \tag{20}$$

we list the cross sections for each channel in Table 3.

The total cross section for double J/ψ production at B-factories up to order $\mathcal{O}(\alpha^2\alpha_s^3)$ is the sum of those for different channels. Note that the two processes which are symmetric in the sense of switching n_1 and n_2 are only counted once to avoid the double counting. We obtain this value as $\sigma = 0.118$ fb. As a comparison, we list the results of

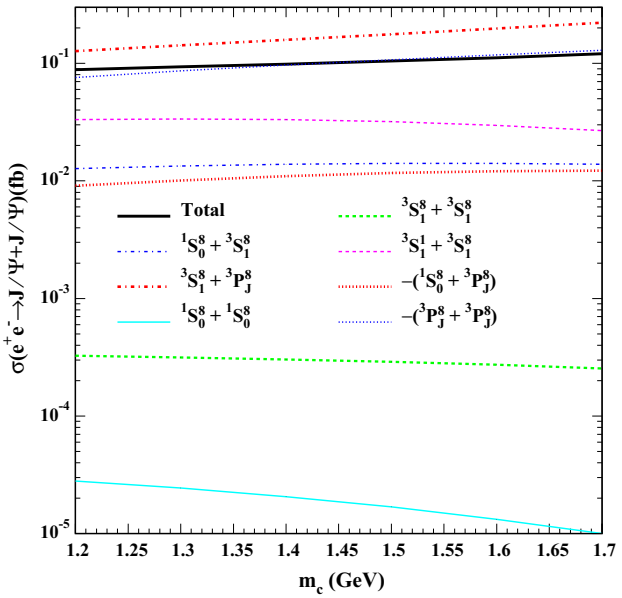

Fig. 2 σ as a function of m_c. The renormalization scale is fixed to $\mu_r = 3.0$ GeV

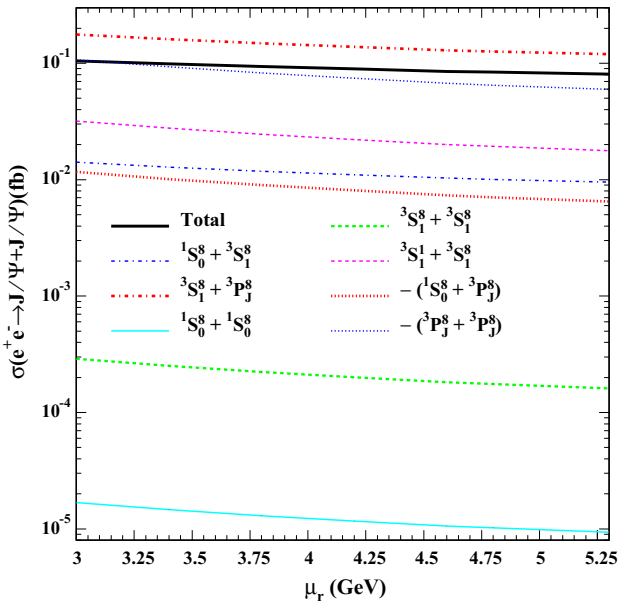

Fig. 3 σ as a function of μ_r. The c-quark mass is fixed to $m_c = 1.5$ GeV

the exclusive double J/ψ production cross sections at B-factories given in Ref. [30]. Adopting different values of m_c and μ_r, the QCD NLO results range from −3.350 to 2.312 fb, comparing with which, our results on the double J/ψ production in association with light hadrons are even smaller. The constraint on the double J/ψ production cross section given in Ref. [24] is $\sigma(J/\psi + \text{res}) \times \mathcal{B}_{>2} < 9.1$ fb, where $\mathcal{B}_{>2}$ denotes the branching fraction for final states with more than two charged tracks. Appar-

Table 4 The total cross sections for the double J/ψ inclusive production in e^+e^- annihilation at B-factory energy employing different sets of the LDMEs. The values of the LDMEs are taken from Refs. [14–16,18]. The first, second and third uncertainties are from the charm mass, the renormalization scale and the uncertainties of the LDMEs.

References	Butenschon, Kniehl [14]	Chao, Ma, Shao, Wang, Zhang [18]	Gong, Wan, Wang, Zhang [15]	Bodwin, Chung, Kim, Lee [16]
$\langle\mathcal{O}^H(^3S_1^{[1]})\rangle$(GeV^3)	1.32	1.16	1.16	
$\langle\mathcal{O}^H(^1S_0^{[8]})\rangle$(GeV^3)	$(3.04 \pm 0.35) \times 10^{-2}$	$(8.9 \pm 0.98) \times 10^{-2}$	$(9.7 \pm 0.9) \times 10^{-2}$	$(9.9 \pm 2.2) \times 10^{-2}$
$\langle\mathcal{O}^H(^3S_1^{[8]})\rangle$(GeV^3)	$(1.68 \pm 0.46) \times 10^{-3}$	$(3.0 \pm 1.2) \times 10^{-3}$	$(-4.6 \pm 1.3) \times 10^{-3}$	$(1.1 \pm 1.0) \times 10^{-2}$
$\langle\mathcal{O}^H(^3P_0^{[8]})\rangle$(GeV^5)	$(-9.08 \pm 1.61) \times 10^{-3}$	$(1.26 \pm 0.47) \times 10^{-2}$	$(-2.14 \pm 0.56) \times 10^{-2}$	$(1.1 \pm 1.0) \times 10^{-2}$
$\sigma(J/\psi)$(fb)	0.019	0.032	-0.013	0.246[a]
Uncertainties(fb)	$\pm 0.007 \pm 0.003 \pm 0.008$	$\pm 0.049 \pm 0.004 \pm 0.007$	$\pm 0.042 \pm 0.014 \pm 0.001$	$\pm 0.35 \pm 0.016 \pm 0.082$

[a] Since the CS LDME was not given in Ref. [16], we adopt the most frequently used value $\langle\mathcal{O}^H(^3S[1]_1)\rangle = 1.16$ GeV^3 in the calculation

ently, our results are consistent with the Belle measurement.

To investigate the uncertainties brought about by the two scales, we vary m_c from 1.2 to 1.7 GeV and μ_r from 3.0 GeV to $\sqrt{s}/2$ and calculate the corresponding total cross sections. When one of these scales varies its value, the other is fixed. Note that the LDMEs used in our calculation are obtained with the configuration $m_c = 1.5$ GeV. When investigating the m_c dependence, we need to take the scaling rule, $\langle O^{J/\psi}(n)\rangle \propto m_c^3$, into account.

The total cross section as a function of the charm-quark mass m_c is presented in Fig. 2. We can see that the $^3S_1^{[8]} +^3 P_J^{[8]}$ and $^3P_J^{[8]} +^3 P_J^{[8]}$ channels provide the largest contributions, while the others have smaller contributions with visible hierarchy. Especially, both the $^1S_0^{[8]} +^3 P_J^{[8]} + g$ and the $^3P_J^{[8]} +^3 P_J^{[8]} + g$ cross sections are negative. The total cross section increases from about 0.09 fb to about 0.15 fb as m_c increases from 1.2 to 1.7 GeV. The μ_r dependence of the total cross section is presented in Fig. 3, and the σ decreases from 0.118 fb to 0.09 fb as μ_r increases from 3.0 GeV to $\sqrt{s}/2$. The dependence on the two scales is not strong, which indicates good convergence of the perturbative expansion.

Since there are several parallel extractions of the LDMEs, we need to investigate the uncertainties brought about by the different values of them. In Table 4, we present the results for four sets of the LDMEs, associated with the uncertainties arising from the variation of m_c and μ_r. The first, second and third uncertainties are from m_c, μ_r and the uncertainties of the LDMEs. The values of the errors presented here are the largest deviation of the cross sections from the default value when one of the parameters vary from its minimum to maximum values, while the other two parameters are fixed. In our calculation, m_c ranges from 1.2 to 1.7 GeV and μ_r ranges from 3.0 GeV to $\sqrt{s}/2 = 5.8$ GeV. As is shown in Table 4, the total cross sections obtained by using the LDMEs in Ref. [16] are almost the double of ours; however, they are still too small to be observed by the experiment.

4 Summary and conclusion

We calculated the total cross sections for double J/ψ production in e^+e^- annihilation at the B-factory energy up to $\mathcal{O}(\alpha^2\alpha_s^3)$ within the framework of NRQCD. We studied the m_c and μ_r dependence of the total cross sections, and found that the results ranges from 0.09 to 0.15 fb. Also, we investigated the uncertainties by trying different sets of the LDMEs. Even for the largest results, the total cross section is too small for Belle to observe any significant access. This result is consistent with the Belle measurement.

Acknowledgements We would like to thank Bin Gong for helpful discussions. This work is supported by the National Nature Science Foundation of China (No. 11405268 and 11647113).

Funded by SCOAP^3.

References

1. G. T. Bodwin, E. Braaten, G. P. Lepage, Phys. Rev. D **51**, 1125 (1995) [Erratum: Phys. Rev. D 55, 5853 (1997)]. arXiv:hep-ph/9407339
2. E. Braaten, S. Fleming, Phys. Rev. Lett. **74**, 3327 (1995). arXiv:hep-ph/9411365
3. Y.-Q. Ma, K. Wang, K.-T. Chao, Phys. Rev. Lett. **106**, 042002 (2011). arXiv:1009.3655 [hep-ph]
4. M. Butenschoen, B.A. Kniehl, Phys. Rev. Lett. **106**, 022003 (2011). arXiv:1009.5662 [hep-ph]
5. Y.-Q. Ma, K. Wang, K.-T. Chao, Phys. Rev. D **83**, 111503 (2011). arXiv:1002.3987
6. H.-F. Zhang, L. Yu, S.-X. Zhang, L. Jia (2014). arXiv:1410.4032
7. L.D. McLerran, R. Venugopalan, Phys. Rev. D **49**, 2233 (1994). arXiv:hep-ph/9309289
8. L.D. McLerran, R. Venugopalan, Phys. Rev. D **49**, 3352 (1994). arXiv:hep-ph/9311205

9. L.D. McLerran, R. Venugopalan, Phys. Rev. D **50**, 2225 (1994). arXiv:hep-ph/9402335
10. Z.-B. Kang, Y.-Q. Ma, R. Venugopalan, JHEP **01**, 056 (2014). arXiv:1309.7337
11. Y.-Q. Ma, R. Venugopalan, Phys. Rev. Lett. **113**, 192301 (2014). arXiv:1408.4075
12. Y.-Q. Ma, R. Venugopalan, H.-F. Zhang, Phys. Rev. D **92**, 071901 (2015). arXiv:1503.07772
13. Y.-J. Zhang, Y.-Q. Ma, K. Wang, K.-T. Chao, Phys. Rev. D **81**, 034015 (2010). arXiv:0911.2166
14. M. Butenschoen, B.A. Kniehl, Phys. Rev. D **84**, 051501 (2011). arXiv:1105.0820
15. B. Gong, L.-P. Wan, J.-X. Wang, H.-F. Zhang, Phys. Rev. Lett. **110**, 042002 (2013). arXiv:1205.6682
16. G.T. Bodwin, H.S. Chung, U.-R. Kim, J. Lee, Phys. Rev. Lett. **113**, 022001 (2014). arXiv:1403.3612
17. M. Butenschoen, B.A. Kniehl, Phys. Rev. Lett. **108**, 172002 (2012). arXiv:1201.1872
18. K.-T. Chao, Y.-Q. Ma, H.-S. Shao, K. Wang, Y.-J. Zhang, Phys. Rev. Lett. **108**, 242004 (2012). arXiv:1201.2675
19. R. Aaij et al., LHCb. Eur. Phys. J. C **75**, 311 (2015). arXiv:1409.3612
20. M. Butenschoen, Z.-G. He, B.A. Kniehl, Phys. Rev. Lett. **114**, 092004 (2015). arXiv:1411.5287
21. H. Han, Y.-Q. Ma, C. Meng, H.-S. Shao, K.-T. Chao, Phys. Rev. Lett. **114**, 092005 (2015). arXiv:1411.7350
22. H.-F. Zhang, Z. Sun, W.-L. Sang, R. Li, Phys. Rev. Lett. **114**, 092006 (2015). arXiv:1412.0508
23. Z. Sun, H.-F. Zhang (2015), arXiv:1505.02675
24. K. Abe et al. (Belle), Phys. Rev. D **70**, 071102 (2004). arXiv:hep-ex/0407009
25. B. Aubert et al. (BaBar), Phys. Rev. D **72**, 031101 (2005). arXiv:hep-ex/0506062
26. G.T. Bodwin, J. Lee, E. Braaten, Phys. Rev. Lett. **90**, 162001 (2003). arXiv:hep-ph/0212181
27. G. T. Bodwin, J. Lee, E. Braaten, Phys. Rev. D **67**, 054023 (2003) [Erratum: Phys. Rev.D72,099904(2005)]. arXiv:hep-ph/0212352
28. K. Hagiwara, E. Kou, C.-F. Qiao, Phys. Lett. B **570**, 39 (2003). arXiv:hep-ph/0305102
29. G.T. Bodwin, E. Braaten, J. Lee, C. Yu, Phys. Rev. D **74**, 074014 (2006). arXiv:hep-ph/0608200
30. B. Gong, J.-X. Wang, Phys. Rev. Lett. **100**, 181803 (2008). arXiv:0801.0648
31. Y. Fan, J. Lee, C. Yu, Phys. Rev. D **87**, 094032 (2013). arXiv:1211.4111
32. K.-Y. Liu, Z.-G. He, K.-T. Chao, Phys. Lett. B **557**, 45 (2003). arXiv:hep-ph/0211181
33. K. Wang, Y.-Q. Ma, K.-T. Chao, Phys. Rev. D **84**, 034022 (2011). arXiv:1107.2646
34. H.-R. Dong, F. Feng, and Y. Jia, JHEP **10**, 141 (2011) [Erratum: JHEP02,089(2013)]. arXiv:1107.4351
35. K. A. Olive et al., Particle Data Group. Chin. Phys. C **38**, 090001 (2014)
36. B. Gong, J.-X. Wang, Phys. Rev. D **77**, 054028 (2008). arXiv:0712.4220
37. T. Hahn, Comput. Phys. Commun. **140**, 418 (2001). arXiv:hep-ph/0012260
38. R. Mertig, M. Bohm, A. Denner, Comput. Phys. Commun. **64**, 345 (1991)
39. A.V. Smirnov, JHEP **10**, 107 (2008). arXiv:0807.3243
40. F. Feng, Comput. Phys. Commun. **183**, 2158 (2012). arXiv:1204.2314
41. J.-X. Wang, Nucl. Instrum. Meth. **A534**, 241 (2004). arXiv:hep-ph/0407058
42. B.W. Harris, J.F. Owens, Phys. Rev. D **65**, 094032 (2002). arXiv:hep-ph/0102128